

Archived at the Flinders Academic Commons

<http://dspace.flinders.edu.au/dspace/>

This is the publisher's copyrighted version of this article.

Copyright (2003) American Institute of Physics. This article may be downloaded for personal use only. Any other use requires prior permission of the author and the American Institute of Physics.

*The following article appeared in Andersson, G., Gommans, H.H., Denier van der Gon, A.W., & Brongersma, H.H., 2003. Liquid metals as electrodes in polymer light emitting diodes. *Journal of Applied Physics*, 93(6), 3299-3307. and may be found at [doi:10.1063/1.1556183](https://doi.org/10.1063/1.1556183)*

Liquid metals as electrodes in polymer light emitting diodes

G. G. Andersson, H. H. P. Gommans, A. W. Denier van der Gon,^{a)}
and H. H. Brongersma

*Department of Applied Physics, Eindhoven University of Technology, P.O. Box 513, 5600 MB Eindhoven,
The Netherlands*

(Received 30 August 2002; accepted 6 January 2003)

We demonstrate that liquid metals can be used as cathodes in light emitting diodes (*p*LEDs). The main difference between the use of liquid cathodes and evaporated cathodes is the sharpness of the metal–polymer interface. Liquid metal cathodes result in significantly sharper metal–organic interfaces than vapor deposited cathodes, due to the high surface energy of the metals. The sharper interface in *p*LEDs with liquid metal cathodes is observed by neutral impact collision ion scattering spectroscopy and low energy ion scattering spectroscopy measurements. The influence of interface sharpness on device performance was studied by comparing current–voltage–light characteristics of devices with OC₁C₁₀ paraphenylenevinylene (PPV) as electroluminescent polymer and indium tin oxide (ITO) as hole injection electrode, and different cathodes. Comparison of devices using a liquid Ga cathode and an evaporated Al cathode showed that light emission for the liquid Ga cathode is two orders of magnitude larger than for the evaporated Al cathode, and that the external light efficiency is increased by an order of magnitude. Since the work function of Ga and Al is nearly the same, the poor performance for evaporated Al LEDs is attributed to the formation of an interfacial layer where Al has diffused into, and reacted with, the PPV. This interfacial layer has poor electrical conduction compared to pure PPV, and contains quenching sites which reduce light emission. Low work function liquid metal cathodes were studied by using liquid Ca and Ba amalgams. The improved performance of liquid amalgam *p*LEDs is attributed to the different structure of the metal–polymer interface. The enormous increase in light and current through the amalgam devices compared to those using pure Hg demonstrate that less than 1 ML of a metal with a low work function at the polymer–cathode interface can have a dramatic effect on the performance of the devices. Devices with a liquid Ca amalgam cathode showed an increase of the current (by 50%) and brightness (80%) compared to devices with an evaporated Ca cathode, which is ascribed to reduced diffusion of Ca into the emissive PPV layer. © 2003 American Institute of Physics.

[DOI: 10.1063/1.1556183]

I. INTRODUCTION

Investigation of the properties of interfaces in polymer light emitting diodes (*p*LEDs) contributes to the fundamental understanding of the functioning of these devices, and can lead to device improvements. Previous research in this area has focused on the chemical interactions at interfaces as well as on charge transport over interfaces.^{1–3} Of special interest is the interface between the electron injecting cathode and the organic emissive layer of the *p*LEDs. The majority of *p*LEDs with a reasonable performance employs metals as cathodes, and the influence of different materials on the electron injection process has been investigated.^{4–6} In by far most cases the metallic cathode is deposited by thermal evaporation or sputter deposition on the organic material directly onto the emissive organic layer, or onto an organic charge transport and electron-injection layer. The deposition is a crucial step in the fabrication process since the metals diffuse into,^{7–9} and interact with, the organic material.^{10–15} Such indiffusion is a general phenomenon in polymer metallization.¹⁶

Previous results on metal deposition on conducting polymers give a picture of some of the processes that may occur upon metal deposition. Fahlman, Brédas, and Salaneck⁸ concluded from x-ray photoelectron spectroscopy (XPS) measurements that during thermal deposition of sodium on poly(2,5,2',5'-tetrahexyloxy-8,7'-dicyano-di-paraphenylenevinylene) (CN-PPV) the metal diffuses uniformly in the detection range of XPS into the polymer layer with the formation of electronic states within the gap. The formation of gap states is also reported for sodium and rubidium deposited on different organic compounds.^{10–13} During thermal deposition of Ca on α,ω -diphenyltetradecaheptane (DP7, which can be regarded as a model substance for PPV), and DHPPV (a PPV derivative), a diffusive layer of the organic material with the metal is formed with an estimated thickness of several nanometers. Also in this case new electronic states are formed in the gap between the highest occupied molecular orbital (HOMO) and the lowest unoccupied molecular orbital (LUMO). During the evaporation of potassium and rubidium on PPV and DP7 the metals diffuse deeper than the detection range accessible with XPS. In these systems electronic states are also formed within the energy gap of the organic materials.

^{a)}Author to whom correspondence should be addressed; electronic mail: a.w.denier.van.der.Gon@tue.nl

The reason for diffusion of the metals into the organic layer during deposition is the high surface energy of the metal compared to that of the organic substrate (typically several 100–1000 mJ/m² for metals, and 20–50 of mJ/m² for organics). Therefore, a metal atom arriving at a polymer surface will rapidly be covered by the polymer in order to reduce its surface energy. When subsequent metal atoms arrive, they will also diffuse into the polymer, but may be trapped by other metal atoms in the subsurface layers. This will reduce diffusion and eventually the metal can stay for long times at the outer surface. The arrival rate of the metal atoms and the temperature will influence the thickness of the distributed metal–polymer interface that is formed.

It has been shown by Greczynski, Salaneck, and Fahlman that a buffer layer can be used to hinder the interaction of metals with organic materials.¹⁷ Hasaki *et al.* showed that a buffer layer of Al between lithium and tris(8-hydroxyquinolino)aluminum (Alq₃) enhances the performance of *p*LEDs.⁴ Note, that after the deposition of an organic material on a metal layer a diffusive layer has also been observed. Huang *et al.* reported that a thin aluminum oxide layer helps to hinder the diffusion of Al into the deposited Alq₃ layer.¹⁸

Here, we introduce an approach to control the metalorganic interface formation. By contacting a liquid metal to the organic layer to form the cathode, the diffusion of the metal into the organic material should be considerably reduced, since the metal does not arrive at the surface as single atoms. In the liquid cathode, the metal atoms are strongly bound together which provides an energy barrier to leave the surface of the metal. Therefore the diffusion of metal into the organic material is expected to be strongly reduced, with a much sharper metalorganic interface as a result. Devices fabricated using this approach should thus better resemble the intrinsic materials properties. In addition, comparison of devices using liquid cathodes and evaporated cathodes with similar work functions allows us to determine the influence of metal diffusion on device performance.

To demonstrate the use of liquid cathodes, and to compare liquid and evaporated cathodes for pure metals, we first use liquid Ga as cathode, and compare the device performance with LEDs using thermally evaporated Al. The work functions of pure Ga and Al are almost the same (4.2 and 4.3 eV, respectively), therefore differences in device performance will be dominated by differences in the metalorganic interface.

Only few pure metals are in the liquid phase close to room temperature, and the choice is effectively limited to gallium and mercury, which both have a high work function. For a good light emission, cathodes are needed which have a low work function. As an alternative for pure liquid metals, we have chosen alkali and earth alkali amalgams. The formation of these amalgams is possible since the metals of the group I and II are soluble in Hg even at room temperature. Since the surface energies of the alkali and alkaline earth metals are much lower than that of Hg, the alkali and alkaline earth elements strongly segregate to the surface and interface.¹⁹ It can be estimated that already at a bulk concentration of about 2×10^{-4} wt% of Ca and Ba, a surface cov-

erage of these alkali and alkaline earth metals of 0.5–1 ML is achieved.¹⁹ A coverage of 0.5–1 ML alkali or alkaline earth metals is sufficient to obtain a work function that is close to the bulk material of the adsorbed metal,²⁰ and the amalgams can thus be used as low work function electrodes. Since the surface energies of metals are much higher than that of organic compounds, the enrichment of the low work function metals at the vacuum–metal interface is nearly the same as that at the metal–organic interface. An important side effect of the doping of the amalgams is that oxides do not diffuse easily through the metal. This will give a purification of the alkali or alkaline earth metal on its way to the interface.

We have fabricated devices with liquid Ca and Ba amalgams, and compare the device characteristics with those of LEDs fabricated using thermally deposited Ca. An additional advantage of liquid metals is that they can easily be removed, which enables surface studies of the remaining polymer side of the interface. Ion scattering techniques have been used to study the metal–organic interfaces, thus allowing a correlation between metal diffusion into the polymeric layer and device performance.

II. EXPERIMENT

The fabrication process of the *p*LEDs with an evaporated metal electrode and the used equipment is described in detail in Ref. 21. Cleaning of the indium tin oxide (ITO) and spin coating of the polymer layer for *p*LEDs with a liquid metal cathode was done in the same way as for the evaporated metal LEDs. The *p*LEDs were fabricated with a 170-nm-thick OC₁C₁₀-PPV layer in the case of the Al and Ga electrodes, and with a 130 nm OC₁C₁₀-PPV layer in the case of the Ca, Hg and amalgam electrodes. Contacting of the polymer layer and device characterization for LEDs with liquid Ga as cathode was performed in the same glovebox as used for spin coating the PPV layer, which has oxygen and moisture levels below 1 ppm. Contacting of the polymer layer with Hg and amalgam metal electrodes, and the measurements of the respective current–voltage–light characteristics was performed in a different glovebox, because of the high vapor pressure of Hg (the high vapor pressure also prohibits direct analysis of Hg samples in UHV analysis techniques). This glovebox uses a flowing nitrogen stream to reduce oxygen and moisture levels to roughly 100 ppm. The samples were transported to the second glovebox after spin coating in a suitcase in order to exclude the contact with air.

In Fig. 1, contacting of the polymer layer with the liquid metals is shown schematically. Four pins were used as contacts to the ITO anode. In order to form the liquid cathode, a droplet of Ga heated to 35 °C or of pure Hg was attached to the PPV surface. Hg electrodes were used as liquid electrodes, whereas Ga electrodes were used after the metal droplet was solidified, which occurred within a few minutes after attaching the droplet. To ensure a clean PPV-metal interface, the droplets were extracted from the center of a larger liquid metal droplet using a pipette, and then immediately deposited on the PPV surface. For the amalgam contacts, a piece of Ca or Ba was immersed into the Hg droplet (after the contact between Hg and the PPV had been made)

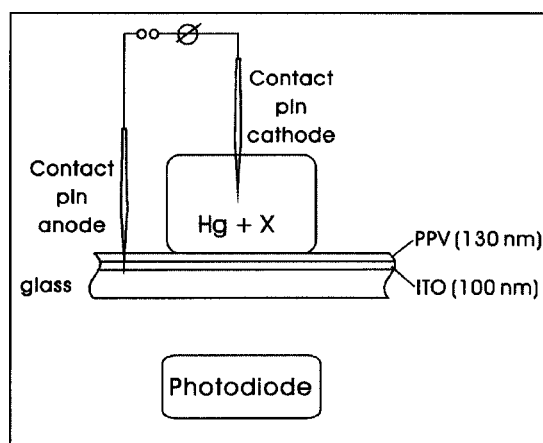


FIG. 1. Schematic of application and electrical characterization of liquid metal cathodes for *p*LEDs. As liquid metals pure Ga, pure Hg, and Ca and Ba amalgams were used.

until a strong reduction of the surface tension of the amalgam could be observed. Before immersing the metals into the Hg, the surface oxide layer of the Ca or Ba was removed in order to enable solving of the metals. The electrical contact to the cathode was performed by immersing a pin into the liquid metal. The active area of the *p*LEDs was about 24 mm² in the case of the Ga and about 16 mm² in the case of the Hg or amalgam cathodes. We also tried to make low work function liquid contacts by using Ca and Ba in combination with Ga, but the solubility of the alkali and alkaline earth elements in Ga proved to be too low.

Ion scattering techniques were used to investigate the modification of the surface and near surface area of the PPV due to the different ways of forming the metal cathode. To study the incorporation of Ga into the PPV surface upon contacting with the liquid metal, low energy ion scattering (LEIS) measurements were conducted on the PPV surface after removal of the Ga droplet. LEIS determines the composition of the outermost atomic layer, however some indication concerning the composition in deeper layers can also be obtained by ion sputtering. The samples were transported in a suitcase under nitrogen atmosphere to the LEIS setup, which is especially suited to study polymers, see, e.g., Ref. 22 for a description. The Ga concentration at the PPV surface was quantified by comparison with the LEIS signal from a liquid metal Ga drop.

Concentration depth profiles of Ca in the PPV after thermal evaporation of the metal on the polymer and after operation of LEDs with amalgam electrodes were determined with neutral impact collision ion scattering spectroscopy (NICISS). Concentration profiles up to a depth of several nanometers with a depth resolution of 0.5–1 nm can be determined. The method and the setup are described in detail in Ref. 23. The applied dose during the measurement was less than 5×10^{13} ions/cm², which ensures that the disorder and damage induced is negligible. The PPV with deposited Ca layer were transported in the dark under nitrogen atmosphere to the NICISS setup and have been in contact with air only for a few minutes during the mounting of the samples in the setup. The samples with an amalgam electrode were trans-

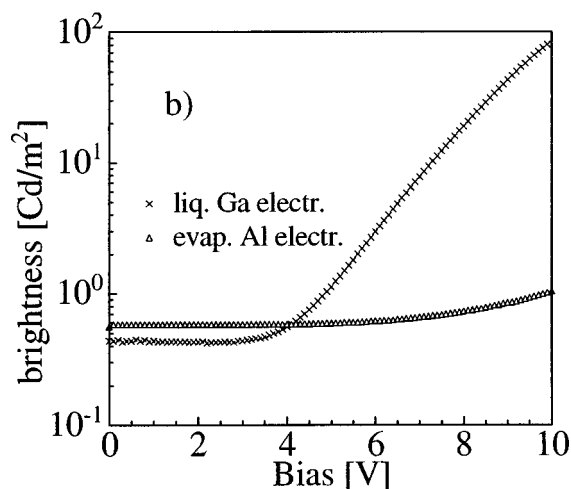
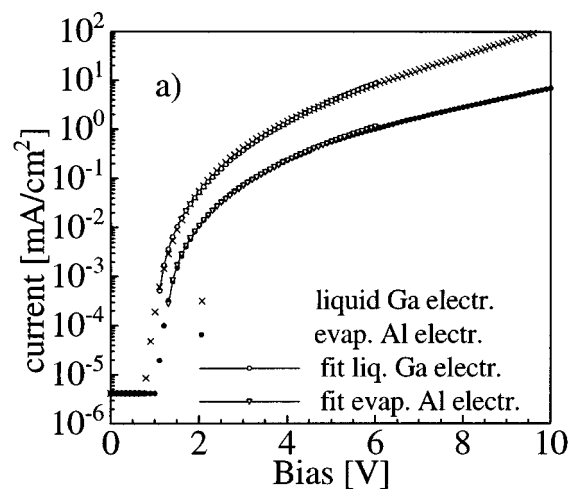


FIG. 2. *I*–*V* (a) and light *V* (b) characteristics of *p*LEDs with cathodes of Ga and Al. Ga was brought into contact as a liquid, while Al was thermally evaporated.

ported in the dark, but in contact with air to the NICISS setup.

III. RESULTS

A. Comparison of liquid Ga and evaporated Al cathodes

In Fig. 2 we show the current density and luminance of a *p*LED with a liquid Ga cathode as measured under forward bias. The smooth *I*–*V* and light *V* curves and low leakage currents at low voltages directly show that good contacts can be made using liquid metals as cathodes. For comparison, the measurements on a *p*LED with an evaporated Al cathode are also shown in Fig. 2. Despite the almost identical work functions for pure Ga and Al, there is a dramatic difference between the current density and light output of the two devices. The current density for the liquid Ga cathode is roughly a factor of 10 higher than for the evaporated Al cathode. Second, whereas for an evaporated Al cathode almost no light emission occurs up to 10 V, the luminance of the liquid Ga *p*LED becomes significant above 5 V, and at 10 V it is almost a factor of 100 more than for the evaporated Al *p*LED.

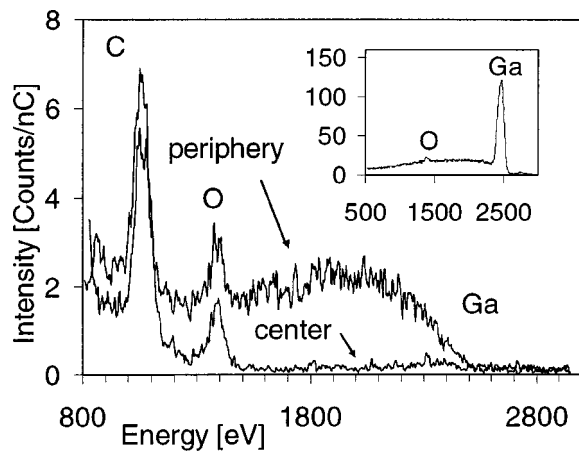


FIG. 3. LEIS spectra of clean OC_1C_{10} -PPV (center) and partly covered with Ga (periphery). The inset depicts a LEIS spectrum of Ga, which is partially covered with oxygen. All spectra are recorded using $3 \text{ keV } ^3\text{He}^+$ ions. The Ga coverage on the PPV surface is almost negligible after removal of the Ga droplet. The spectrum marked with periphery was measured close to the periphery of the Ga droplet, where oxidation of the Ga has occurred.

To investigate in more detail the difference between the devices, the I - V curves were fitted using the model described by Davids, Campbell, and Smith in Ref. 24. This model was especially developed to describe I - V characteristics in which one charge carrier is dominant. The model takes into account charge injection (both tunneling and thermionic emission), transport and space charge effects. Image force barrier lowering and interfacial recombination are also included. The fits are shown in Fig. 2, and apparently a good description of the I - V curves is obtained using this model. We use a dielectric constant $\epsilon=3$ and assumed that the effective mass of both holes and electrons equals the electron rest mass. The density of conjugated chain segments times the number of ways that a chain can be occupied, n_0 , is set equal to 10^{21} cm^{-3} .²⁴ The parameters used for fitting our device currents were the hole energy barrier Φ_h , built-in potential V_{bi} , the hole mobility μ_0 and the term γ which accounts for the field dependence of the mobility of the form $\mu = \mu_0 \exp(\gamma\sqrt{E})$, with E the electric field strength. Compared to Φ_h the energy barrier for electron injection Φ_e was much higher and therefore the model electron current is negligible. The remaining parameters describing the electron current are only important as far as they effect the hole parameters just mentioned. For Ga we obtained $\Phi_h = 0.4 \pm 0.1 \text{ eV}$, $V_{bi} = 1.0 \pm 0.1 \text{ V}$, $^{10}\log \mu_0 = -9.8 \pm 1$ (μ_0 in m^2/Vs) and $^{10}\log \gamma = -3.3 \pm 0.3$ (γ in $[\text{m/V}]^{1/2}$) and for Al $\Phi_h = 0.4 \pm 0.1 \text{ eV}$, $V_{bi} = 1.2 \pm 0.1 \text{ V}$, $^{10}\log \mu_0 = -10 \pm 1$ (μ_0 in m^2/Vs) and $^{10}\log \gamma = -3.7 \pm 0.3$ (γ in $[\text{m/V}]^{1/2}$). The resulting values are in reasonable agreement with those available in literature for similar systems.

In order to study the interface between the liquid Ga cathode and the PPV, we removed the Ga droplet and examined with LEIS the PPV surface which was previously in contact with Ga. In case the metal is highly reactive, direct bonding to the polymer as well as the formation of carbidic or oxidic compounds is possible²⁵ and its residue after bulk removal should be detected at the surface. In Fig. 3 we show the LEIS spectra obtained after removal of the Ga droplet,

and in the inset a Ga reference spectrum is also shown. At the center of the contact area the Ga signal could hardly be detected, indicating an extremely small Ga concentration at the PPV surface after contact, which was estimated by calibration to be less than <0.5 at %. The LEIS spectra also indicate that very little Ga has diffused into the PPV, since this would show up as intensity below the surface peak energy in the LEIS spectra. The carbon and oxygen intensities were identical to that of a clean OC_1C_{10} PPV surface, also indicating that the PPV surface after contact was not disrupted. However, at the periphery of the droplet we indeed observed macroscopic remnants by eye, and a large Ga signal was observed in the LEIS spectrum obtained from this area. The large signal just below the surface peak energy of Ga ($<2500 \text{ eV}$) indicates that a significant amount of Ga is incorporated into the PPV surface in the peripheral area. Thus, in the area close to the N_2 atmosphere in the glovebox, the Ga has reacted, presumably due to the presence of oxygen and/or moisture at the level of 1 ppm. These levels are still high enough to cause considerable oxidation over time. It should be noted that the light emission mainly originated from the center of the droplet contact area, and thus the light emission is not caused by this reacted area.

B. Comparison of liquid amalgam cathodes and evaporated Ca cathodes

In Fig. 4, I - V and light V characteristics are shown for pLEDs with an evaporated Ca cathode, a pure liquid Hg cathode, and a liquid Ca amalgam cathode. The characteristics for the liquid Hg cathode are similar to that of devices with an evaporated gold cathode,²⁶ where the current is dominated by holes. The work function of Hg is 4.49 eV which, although lower than for gold, is apparently still high enough to prevent the injection of electrons into the PPV, and as a consequence luminescence is not observed for voltages up to 14 V.

The characteristics of the device with liquid Ca amalgam are very different from those using a pure liquid Hg cathode, indicating that the Ca is indeed dissolved into the Hg, and segregates to the interface (as also observed from the surface tension of the liquid drop). The onset of the current for liquid Hg is 0.75 V, which increases to 1.35 V for the Ca devices. Also, the slope of the I - V characteristic is much higher for the Ca amalgam cathode. Finally, the LEDs with a pure liquid Hg cathode did not emit light at voltages below 14 V, whereas liquid Ca amalgam devices show a light onset already around 2 V. These observations are consistent with a high work function of the liquid Hg cathode, and a subsequent lowering of the work function upon segregation of Ca to the interface.

The onset voltage for current and for light emission is nearly the same for the liquid Ca amalgam and the evaporated Ca cathode, although closer inspection shows that the onsets for current and light emission are both 0.25 V lower for the Ca amalgam. Although the lower current-onset voltage would indicate a slightly higher work function for the liquid Ca amalgam cathode, the lower onset for light emission points in the opposite direction, and the difference can

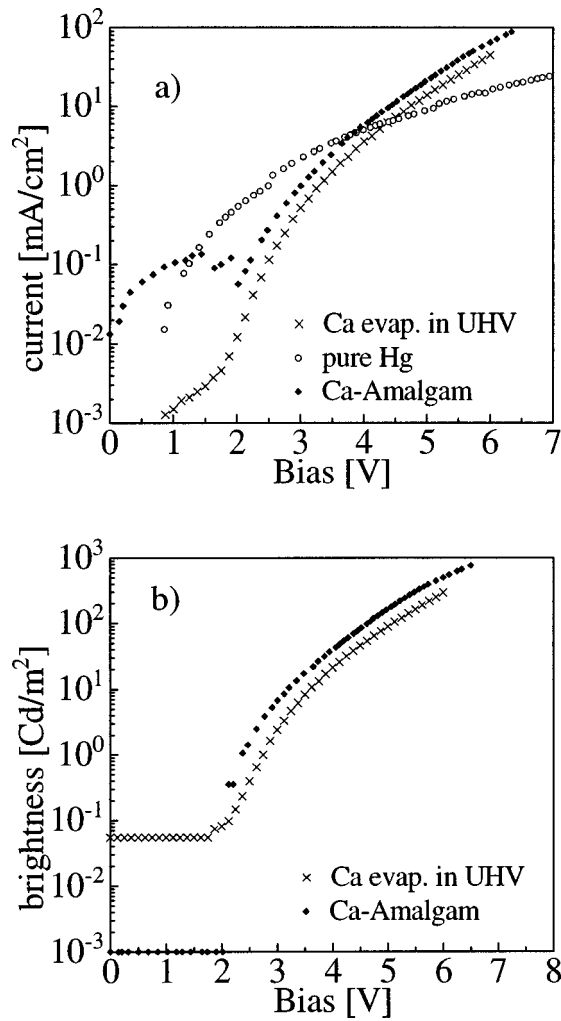


FIG. 4. I - V (a) and light V (b) characteristics of p LEDs with evaporated Ca, pure liquid Hg, and liquid Ca amalgam cathodes. The onset for the emission of light of the LEDs with pure Hg as cathode was at about 14 V.

thus not simply be attributed to a different work function, but must be related to the interface formation.

The current for the devices with Ca amalgam is about 50% higher than for those with an evaporated Ca cathode; at the same time, the brightness is about 80% increased. Thus the slopes of the external efficiency, which are shown in Fig. 5, are also similar but the values for the Ca amalgam device are higher than that of the evaporated Ca layer. At voltages lower than the light-emission onset voltage the Ca amalgam devices have a reproducible but unusual high current. The high current is found not to depend on if the current is reduced from higher voltages to zero, or if it is increased from zero voltage.

In Fig. 6 the characteristics of Ca amalgam and Ba amalgam devices are shown. Clearly, the Ba amalgam device has a much higher current for low voltages, which increases linearly with voltage below 4.5 V, see inset in Fig. 6. This linear increase at low voltages is an indication for leakage currents, which may be induced by Ba diffusion into the PPV. For higher voltages, the increase in current for the Ca amalgam becomes larger, and finally the current for the Ca amalgam devices is higher than for the Ba amalgam.

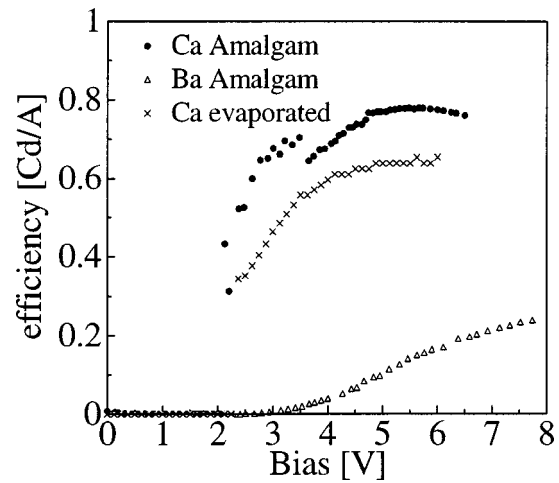


FIG. 5. Efficiency of p LEDs with cathodes of Ca amalgam, Ba amalgam and an evaporated Ca layer.

In contrast to the strong difference in I - V characteristics, the shape of the light V characteristics of the Ba amalgam device is not very different from the Ca amalgam device. This shows that the formation of an amalgam and low-work function interface formation also works for the Ba.

It is worth noting that the Ba and the Ba amalgam oxidized much faster than the Ca and the Ca amalgam, due to its

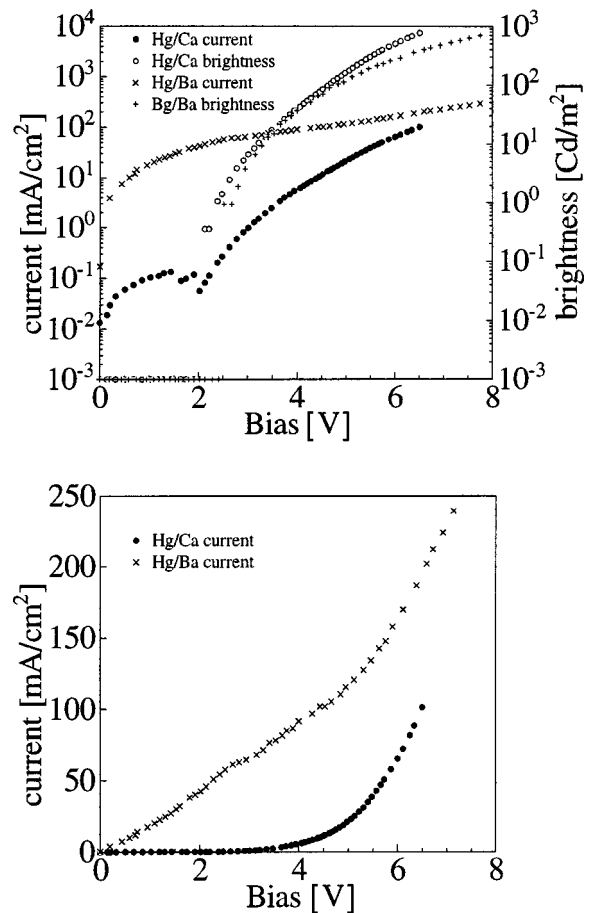


FIG. 6. Upper panel: I - V and light V characteristics of p LEDs with cathodes from Ca amalgam and Ba amalgam. Lower panel: I - V characteristics on a linear scale.

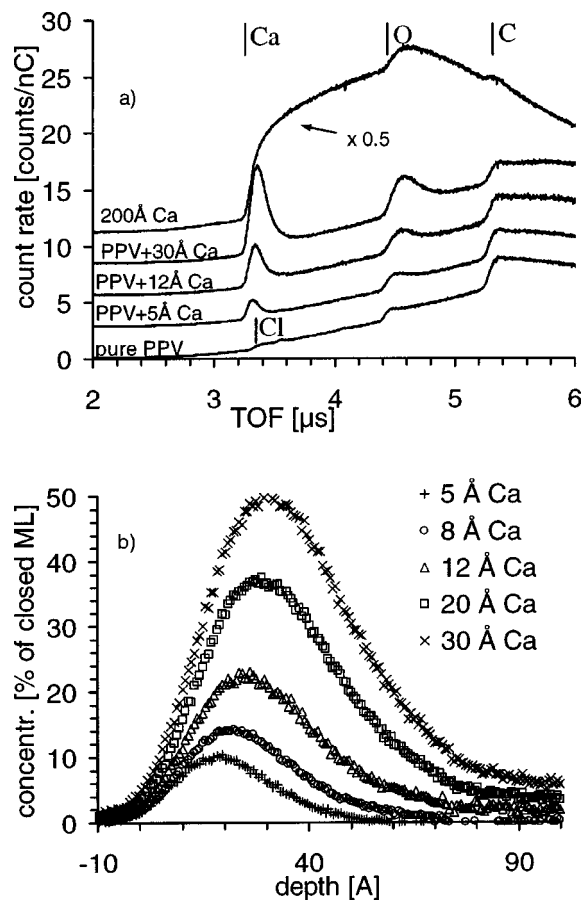


FIG. 7. Time of flight NICISS measurements of a pure PPV layer and those with Ca of different thickness deposited on PPV (a), and the related concentration depth profiles of Ca (b). The spectrum of the sample with 200 Å Ca deposited on PPV is multiplied with a factor of 0.5. Offsets are added to the curves in (a) for clarity.

higher reactivity with oxygen and water. During operation, the Ca amalgam devices showed a decrease of the current density some time after performing the contact of the amalgam with the polymer layer. At the same time the area from which light was emitted was shrinking due to oxidation of the amalgam in that area. The oxidation of the amalgam would be strongly reduced in a glovebox with a much lower oxygen and moisture level, or a suitable encapsulation. We found that the shrinking of the active area of the Ba amalgam devices was faster than that of the Ca amalgam devices, consistent with faster oxidation of the Ba from the glovebox environment.

C. Concentration depth profiles of Ca in PPV

We studied the interface formation for evaporated Ca layers on PPV by depth profiling with NICISS. In Fig. 7 we show NICISS spectra and the resulting Ca depth profiles for different amounts of Ca deposited onto the PPV, and also for a pure PPV film. Note that the spectrum with a deposited Ca thickness of 200 Å is multiplied by 0.5. In the spectrum of pure PPV a small amount of chlorine is visible, which is an impurity of about 0.2 at. % left during the fabrication process in the PPV.²⁷ The Ca signal increases with increasing amount of evaporated metal, as expected. The shape of the Ca feature

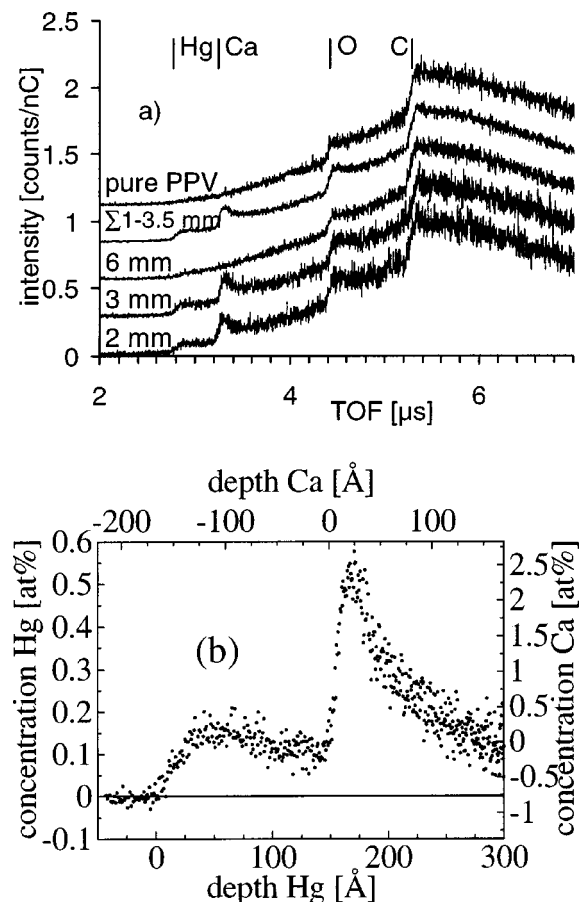


FIG. 8. Time of flight NICISS measurements (a) of PPV layer after the operation in a pLED with an amalgam electrode and concentration depth profiles (b) of Hg and Ca derived from the spectra in (a). The Hg depth profile is nearly constant with respect to the depth and the Ca depth profile shows a pronounced maximum close to the PPV surface at a depth of about 10 to 20 Å. The amalgam was in contact with the polymer in an area with a radius of approximately 3 mm. The measurements were performed on rings with the center in the middle of the area which was in contact with the amalgam. The coincidence of the center of the ring and the middle of the amalgam contact area was about 1 mm. Offsets are added to the curves in (a) for clarity.

shows that for deposited amounts of up to 30 Å the Ca is located in the outermost region of the PPV. The increase of the oxygen signal in the outermost region with increasing Ca deposition is attributed to reaction of Ca with air during sample mounting in the NICISS setup. For the highest amount of deposited Ca (200 Å), the Ca signal is a step with approximately constant height, which indicates that the Ca formed a closed overlayer for this thickness. The Ca signal corresponds to a concentration of about 20 at. % which is consistent with the reaction of the Ca with air to CaCO_3 . In contrast, the spectra up to 30 Å Ca indicate that a closed Ca layer has not been formed, as evidenced by the significantly lower Ca signal height compared to the spectrum for 200 Å. In addition, the depth of maximum Ca concentration shifts from about 15 Å for a deposited amount of 5 Å, to 25 Å for a deposited amount of 30 Å, while at the same time the full width at half maximum of the Ca concentration increases.

NICISS spectra of PPV after contact (and operation as LED) with Ca amalgam are shown in Fig. 8(a) for different positions with respect to the center of the amalgam contact

area, and also for a pure PPV sample. The spectra for amalgam contacted PPV show features due to Hg and Ca atoms in the sample, which are not present in the untreated PPV film. In Fig. 8(b) we show the Hg and Ca depth profile as measured in the center of the amalgam contact area. The Ca concentration reaches a maximum at a depth of about 20 Å, which is similar to the case of evaporated Ca. However, at this depth the concentration is only about 2 at. %. Since the Ca in this case has also reacted to CaCO₃, the Ca coverage corresponds to 10% of a closed monolayer. The difference between the concentration depth profiles for both methods of contacting the polymer is thus mainly in the amount of metal penetrating into the polymer. The Ca concentration is about an order of magnitude lower for the liquid metal contact than for the thermally deposited electrode. The Hg concentration in the PPV varies much less with depth, and shows a nearly constant concentration of about 0.1 at. % up to a depth of 150 Å. A few Hg droplets were observed with an optical microscope on the Hg contacted PPV samples, and we attribute the Hg features in the spectra to these droplets.

IV. DISCUSSION

A. Liquid Ga versus evaporated Al cathodes

Comparison in LED performance between liquid Ga and evaporated Al devices reveals almost two decades of difference in luminance intensity and one decade in efficiency, both in favor of the liquid Ga cathode. It is generally believed that enhanced efficiencies are obtained by balancing the electron and hole currents, since this will shift the recombination zone away from the cathode where quenching might²⁶ occur. The small difference in the work function of Ga and Al has little influence on the current balance, and thus cannot explain the huge increase in luminance and efficiency. (Calculations according to the model described above in Ref. 24 show that a decreased electron injection barrier even results in a slightly diminished current as a result of the increased built-in potential.)

Since the difference in the LED performance cannot be explained by the different electronic properties (work functions) of the metals, the method of interface formation is the most likely cause. Not much is known about the interaction between Ga and PPV, but it was shown by photoelectron spectroscopy that Ga exhibits only weak reactivity with Alq₃.²⁸ The LEIS measurements on the PPV surface after Ga contact show that very little Ga diffuses into the PPV surface, indicating formation of a sharp, well-defined interface. In contrast, it was shown by photoelectron spectroscopy that Ga diffuses into the organic material after being evaporated.²⁸ For evaporation of Al onto PPV, it is known that significant diffusion and interaction between the Al and PPV occurs.²⁹ Our *I*-*V* characteristics also point in this direction. In case of Ga, the built-in potential calculated as the difference in Fermi level between the positive and negative electrode amounts to 0.6 eV, which corresponds reasonably well to the current onset of 0.8±0.1 V. In this calculation the Fermi level of ITO was taken as 4.8 eV³⁰ and vacuum level alignment between ITO and PPV was assumed. This suggests that even if the Ga and PPV interact, the interface

pinning is negligible. In contrast, for Al the calculated built-in potential and experimentally observed current onset are 0.5 and 1.0±0.1 V respectively. The discrepancy between these values we attribute to the formation of a poorly conducting interfacial layer near the cathode, which creates an extra barrier for charge carrier transport, for instance, by a shift of the vacuum level of the PPV with respect to that of the cathode. The assumption of a barrier for the charge transport is supported by angle-resolved XPS measurements on thermally evaporated Al at PPV and MEH-PPV surfaces,²⁹ where the formation of an Al oxide layer was observed in the initial stages of evaporation. Only upon further deposition this was followed by formation of metallic Al. The authors proposed that oxygen atoms of the alkoxy side chains cause the interfacial reaction with Al. Interface pinning cannot explain the difference in the observed currents and merely reduces the built-in potential.³¹ From the angle dependence of the XPS signals, it was concluded that Al fairly diffuses into the PPV for the first 10 ML.²⁹

Fitting the *I*-*V* curves the only parameter that accounts for a major distinction in current is γ , which is 2×10^{-4} (m/V)^{1/2} for Al and 5×10^{-4} (m/V)^{1/2} for Ga. The value of the Ga devices resembles the commonly quoted value for intrinsic conduction in OC₁C₁₀ PPV,³² whereas that of the Al devices is significantly smaller. This seems surprising, since the size of γ normally scales with the amount of disorder, but it is unlikely that evaporation of an aluminum layer induces ordering within the polymer layer. In addition, a reduced γ should be accompanied by an increase of the conductivity³³ due to a reduction in the distribution of the energy levels in the HOMO. In contrast we find in our devices a reduced conductivity. In our opinion the reason for this contradiction is based in a shortcoming of the device model, since it assumes only one, homogeneous, polymer layer. The intention of our article is to emphasize that, due to the penetration of the metal into the polymer, an interface layer is formed, which has different properties than the pure polymer itself, and strongly influences the device properties. Thus the smaller γ may be regarded only as an indication for the reduced conductivity due to the formation of a poorly conducting interface layer between the Al and the PPV. An attempt to derive the cause for the reduced conductivity would require an extended model including at least an additional layer at the interface, and in addition temperature dependent measurements. The much lower luminescence of the Al devices is most likely caused by quenching sites formed during the reaction of the Al with the PPV in the interfacial layer.

B. Ca and Ba amalgam electrodes versus evaporated Ca cathodes

The LEDs with amalgam and evaporated Ca contacts differ very little in work function of the electrode, since the work function of a single alkali or alkaline earth layer adsorbed on other metals is close to that for a thick layer.²⁰ Consequently, the observed differences in device characteristics must be caused by the interface formation. The NICISS measurements showed that Ca diffuses several nm into the PPV layer, when the Ca is deposited by thermal evaporation. For the Ca amalgam contact we found the same depth distri-

bution but the total concentration of Ca in the PPV is strongly reduced. We conclude that higher current, brightness and efficiency for the Ca amalgam LEDs must be attributed to the lower Ca concentration into the PPV.

The observation that also for the Ca amalgam contacts there is still diffusion of Ca into the PPV needs some consideration, since the diffusion of the metal atoms is not expected based on the differences in the surface energies. This indicates that the cost in surface energy of the metal is compensated by a gain in energy when the Ca penetrates into the polymer. The formation of Ca carbide as described in Ref. 25 presents a possible reaction mechanism for this. The enthalpy for the formation of calcium carbide is -62.7 kJ/mol,³⁴ whereas the Ca–Hg binding energy is 57 kJ/mol.³⁵ Thus there is a small gain of energy for the formation of calcium carbide. The much lower Ca concentration for the Ca amalgam cathode thus indicates that there is a significant energy barrier to overcome for this reaction hindering the Ca carbide formation, which is the Ca–Hg binding energy.

Next, we consider the possible influence of Ca diffusion into the PPV on the LED performance. Ultraviolet photoelectron spectroscopy experiments have shown that new states are formed in the gap between HOMO and LUMO upon Ca penetration into PPV.^{15,36} These gap states were attributed to the interaction of Ca with the PPV. Since gap states are able to act as traps for electrons, they reduce the electron transport in the diffusive layer. Blom and deJong²⁶ have shown that charge transport in PPV based LEDs is space charge limited and that the density of traps for electrons is an important parameter. By modeling of the efficiency of the devices they found that the electrons are trapped in a layer of about 10 nm thickness close to the electron injection contact, i.e., the Ca–PPV interface. Thus the reduction of the number Ca atoms interacting with the PPV, as observed for the liquid Ca amalgam cathodes, should increase the current, in agreement with our observations.

Another explanation for the higher current for the Ca amalgam electrodes can be found in the possible oxidation of the PPV upon reaction of Ca with the polymer. We have recently observed the formation of Ca carbide during deposition of Ca on PPV, which is chemically unstable and able to react with oxygen.²⁵ This reaction causes a loss of the π -conjugated structure of the polymer backbone, which also reduces the charge transport in the PPV layer close to the metal–polymer interface. Possible sources of oxygen are oxygen solved in the PPV during the processing of the polymer, or oxygen present during the evaporation process. Reducing the number of Ca atoms in the PPV is thus expected to reduce the loss of the π -conjugated structure, which could also explain the increase in current. However, since a strong reduction of the charge transport occurs only if the Ca–PPV interface is exposed to a high oxygen dose, the creation of gap states and traps for electrons is probably the most important cause for the reduced current for thermally evaporated Ca.

The brightness for Ca amalgam cathode devices increased more than the current, compared to LEDs with evaporated Ca cathodes. A major influence of a difference in reflectivity between Hg and Ca on the brightness of the de-

vices can be excluded, since the reflectivity is even slightly smaller for Hg than for Ca.^{37,38} The reason for the difference in the brightness is in the difference of the number of quenching sites in the devices. It has been shown that gap states act as quenching sites, and reduce the brightness of LEDs.¹⁵ Thus the reduced number of Ca atoms in the PPV for the Ca amalgam cathode should increase the brightness of the devices by decreasing the number of nonradiative recombinations of charge carriers. Since the recombination zone of the charge carriers is close to the metal–polymer interface, reduction of the number of quenching sites in this area will increase the brightness significantly.

Finally, we would like to point out that the influence of Ca diffusion into PPV on LED performance cannot be overcome by simply exposing the PPV–Ca interface to oxygen. Although this reduces the number of quenching sites as shown by Park *et al.*¹⁵ in photoluminescence experiments, it also causes a loss of the π -conjugated structure. Thus the oxidation of the quenching sites leads not to an increase in brightness in the electroluminescence of devices, but to the total device failure as we have shown recently.²¹

V. CONCLUSIONS

We have demonstrated that it is possible to fabricate *p*LEDs using liquid metals as the electron injection electrode. Comparing the depth profiles measured in the near-surface area of the PPV on devices after attaching the liquid metal with those obtained after thermal evaporation of the metal, we found that the diffusion of metal atoms into the PPV is much less for the liquid metal contacts, as expected on the basis of surface energy considerations. This gives us the opportunity to study the influence of the formation of gap states on the charge transport. Until now, this could not be studied since there was no fabrication method which was able to suppress the penetration of the metal atom into the PPV without introducing a new layer of a different material at the metal–PPV interface.

A comparison of liquid metal cathodes with devices employing evaporated metal cathodes with similar work functions shows that the liquid metal cathodes in general have better characteristics, as evidenced by increases in current, brightness and efficiency. This was found both for high work function cathodes (liquid Ga versus evaporated Al) as well as for low work function cathodes (Ca amalgams versus evaporated Ca cathodes). We have shown that the interaction of the metal atoms with the polymer can lead to the formation of an interfacial layer with poor conductivity and quenching sites. Therefore, minimizing the diffusion of metal atoms into the polymer increases current and brightness for *p*LEDs.

For future research, it should be pointed out that the use of liquid metal electrodes is in general a promising concept to study in more detail the influence of the metal polymer interaction on the characteristics and electronic properties of *p*LEDs. Liquid metal electrodes may be removed after the LED has been operated for some time, which offers the possibility of studying the metal–polymer interface using surface science techniques.

ACKNOWLEDGMENTS

The authors gratefully acknowledge Martijn Kemerling for discussions and for making available his modeling software. This work has been sponsored by grants from the Dutch Foundation for Fundamental Research (FOM).

- ¹W. R. Salaneck and M. Löglund, *Polym. Adv. Technol.* **9**, 419 (1998).
- ²H. Ishii, K. Sugiyama, E. Ito, and K. Seki, *Adv. Mater.* **11**, 605 (1999).
- ³M. Stöbel, J. Staudigel, F. Steuber, J. Simmerer, G. Wittmann, A. Kanitz, H. Klausmann, W. Rogler, W. Roth, J. Schumann, and A. Winnacker, *Phys. Chem. Chem. Phys.* **1**, 1791 (1999).
- ⁴E. Hasakl, A. Curioni, P. Seidler, and W. Andreoni, *Appl. Phys. Lett.* **71**, 1151 (1997).
- ⁵M. Stoessel, J. Staudigel, F. Steuber, J. Simmerer, G. Wittmann, A. Kanitz, H. Klausmann, W. Rogler, W. Roth, J. Schumann, and A. Winnacker, *Phys. Chem. Chem. Phys.* **1**, 1791 (1999).
- ⁶S. Karg, M. Meier, and W. Riess, *J. Appl. Phys.* **82**, 1951 (1997).
- ⁷P. Dannetun, M. Fahlman, C. Fouquet, K. Kaerijama, Y. Sonoda, R. Lazaroni, J.-L. Brédas, and W. R. Salaneck, in *Organic Materials for Electronics: Conjugated Polymer Interfaces with Metals and Semiconductors*, edited by J.-L. Brédas, W. R. Salaneck, and G. Wegener (North-Holland, Amsterdam, 1994), p. 113.
- ⁸M. Fahlman, J.-L. Brédas, and W. R. Salaneck, *Synth. Met.* **78**, 237 (1996).
- ⁹M. Stöbel, G. Wittmann, J. Staudigel, F. Steuber, J. Blässing, W. Roth, H. Klausmann, W. Rogler, and J. Simmerer, *J. Appl. Phys.* **87**, 4467 (2000).
- ¹⁰T. Osada, P. Barta, N. Johansson, Th. Kugler, P. Bröms, and W. R. Salaneck, *Synth. Met.* **102**, 1103 (1999).
- ¹¹G. Iucci, M. Löglund, C. W. Spangler, and W. R. Salaneck, *Synth. Met.* **76**, 209 (1996).
- ¹²G. Iucci, K. Xing, M. Löglund, M. Fahlman, and W. R. Salaneck, *Chem. Phys. Lett.* **139**, 244 (1995).
- ¹³M. Löglund, P. Dannetun, S. Stafström, W. R. Salaneck, M. G. Ramsey, C. W. Spangler, C. Frederiksson, and J. L. Brédas, *Phys. Rev. Lett.* **70**, 970 (1993).
- ¹⁴V.-E. Choong, Y. Park, B. R. Hsieh, and Y. Gao, *J. Phys. D* **30**, 1421 (1997).
- ¹⁵Y. Park, V.-E. Choong, B. R. Hsieh, C. W. Tang, and Y. Gao, *Phys. Rev. Lett.* **78**, 3955 (1997).
- ¹⁶F. Faupel, T. Strunskus, M. Keine, A. Thran, C. v. Bechtolsheim, and V. Zaporozhchenko, *Mater. Res. Soc. Symp. Proc.* **511**, 19 (1998).
- ¹⁷G. Greczynski, W. R. Salaneck, and M. Fahlman, *Appl. Surf. Sci.* **175**, 319 (2001).
- ¹⁸M. B. Huang, K. McDonald, J. C. Keay, Y. C. Wang, S. J. Rosenthal, R. A. Weller, and L. C. Feldman, *Appl. Phys. Lett.* **73**, 2914 (1998).
- ¹⁹L. Convers, *J. Chem. Phys.* **36**, 175 (1939).
- ²⁰P. Rudolf, C. Astaldi, A. Bianco, and S. Modesti, *Phys. Rev. B* **47**, 4123 (1993).
- ²¹G. G. Andersson, M. P. de Jong, G. J. J. Wiannds, A. W. Denier van der Gon, L. J. van IJzendoorn, H. H. Brongersma, and M. J. A. de Voigt, *J. Appl. Phys.* **90**, 1376 (2001).
- ²²M. W. G. Ponjée, M. A. Reijme, A. W. Denier van der Gon, H. H. Brongersma, and B. M. W. Langeveld-Voss, *Polymer* **43**, 77 (2002).
- ²³G. Andersson and H. Morgner, *Surf. Sci.* **405**, 13 (1998).
- ²⁴P. S. Davids, I. H. Campbell, and D. L. Smith, *J. Appl. Phys.* **82**, 6319 (1996).
- ²⁵G. G. Andersson, W. J. H. van Gennip, J. W. Niemantsverdriet, and H. H. Brongersma, *Chem. Phys.* **278**, 159 (2002).
- ²⁶P. W. M. Blom and M. J. M. de Jong, *IEEE Sel. Top. Quantum Electron.* **4**, 105 (1998).
- ²⁷G. Andersson, H. H. Brongersma, A. W. Denier van der Gon, L. J. van IJzendoorn, M. P. de Jong, and M. J. A. de Voigt, *Synth. Met.* **113**, 245 (2000).
- ²⁸M. Probst and R. Haight, *Appl. Phys. Lett.* **70**, 1420 (1997).
- ²⁹M. Altreya, S. Li, E. T. Kang, K. G. Neoh, Z. H. Ma, and K. L. Tan, *J. Vac. Sci. Technol. A* **17**, 853 (1999).
- ³⁰T. Osada, Th. Kugler, P. Bröms, and W. R. Salaneck, *Synth. Met.* **96**, 77 (1998).
- ³¹L. H. Campbell, T. W. Hagler, and D. L. Smith, *Phys. Rev. Lett.* **76**, 1900 (1996).
- ³²P. W. M. Blom, M. J. M. Blom, and M. G. van Munster, *Phys. Rev. B* **55**, R656 (1997).
- ³³H. C. F. Martens, P. W. M. Blom, and H. F. M. Schoo, *Phys. Rev. B* **61**, 7489 (2000).
- ³⁴Selected Values of Chemical Thermodynamic Properties, Circular of the National Bureau of Standards, Washington, 1959
- ³⁵K. Hilpelt, *Ber. Bunsenges. Phys. Chem.* **87**, 818 (1983).
- ³⁶W. R. Salaneck and M. Löglund, *Polym. Adv. Technol.* **9**, 419 (1998).
- ³⁷H. Lowery and R. L. Moore, *Philos. Mag.* **13**, 938 (1982).
- ³⁸H. M. O'Brian, *J. Opt. Soc. Am.* **26**, 122 (1936).